Reactivity of cobalt(II)-dichalcogenide complexes: correlation between redox conversion and ligand-field strength

Marvelous, C.

Chapter 4

Redox-conversion Reactivity of The Chalcogen Family: Selenium vs Sulfur

The synthesis is described of the selenium-based ligand L^1SeSeL^1 (2,2'-diselanediylbis(N,N-bis(pyridin-2-ylmethyl)ethan-1-amine) along with its reactivity with cobalt(II) salts. The cobalt(II)-diselenide complex $[Co_2(L^1SeSeL^1)Cl_4]$ was obtained in good yield, and its spectroscopic properties closely resemble that of its sulfur analog. Reaction of L^1SeSeL^1 with Co(II) thiocyanate results in the formation of the cobalt(III) compound $[Co(L^1Se)(NCS)_2]$, similar to reaction of L^1SSL^1. The redox-conversion reactions from the Co(II)-diselenide compound $[Co(L^1SeSeL^1)Cl_4]$ to Co(III)-selenolate complexes $[Co(L^1Se)(MeCN)_2](SbF_6)_2$ and $[Co(L^1Se)(quin)]Cl$ were achieved in a good yield using external triggers such as removal of the halide ions or the addition of the strong-field ligand 8-quinolinolate. Our computational studies show that the ligand-field strength of selenium compounds is smaller than their sulfur analogs, indicating that redox-conversion of cobalt(II)-diselenide into cobalt(III)-selenolate complexes may be more arduous than for the related sulfur compounds.

4.1. Introduction

Electron-transfer reactions frequently occur in biological systems, usually involving transition-metal ions in metalloenzymes.[1-3] Selenium is used in biomimetic studies as an analog for sulfur, as selenium is present in nature in the amino acid selenocysteine, often resulting in enhanced reaction rates compared to cysteine-containing enzymes.[4-7] The redox chemistry of selenium compounds is known to be similar to their sulfur analogues, for example the reduction of the diselenide bond into selenolate ions. Additionally, selenium compounds can participate in faster thiol/disulfide-like exchange reactions,[8] which is an indirect consequence of the more nucleophilic properties of these selenium compounds under neutral conditions.[9]

In the past decade, the redox-conversion reaction of metal-thiolate and metal-disulfide compounds has gathered a lot of interest. The study of the redox-conversion reaction of thiolate and disulfide compounds may provide mechanistic understanding on electron-transfer reactions catalyzed by metalloenzymes. Some reported examples concern the redox-conversion of copper(I)-disulfide vs copper(II)-thiolate complexes and cobalt(II)-disulfide vs cobalt(III)-thiolate complexes.[10, 11] The redox-conversion of cobalt(II)-disulfide to cobalt(III)-thiolate is particularly interesting for several reasons. First of all only few examples have been reported on this matter and expansion of the scope will be helpful to gain more understanding. Additionally, the reactivity of specific disulfide ligands is a point of interest as slightly different ligands may result in a different outcomes. For example, it has been reported that the ligand L^1SSL^1 upon reaction with $Co(SCN)_2$ results in formation of a cobalt(III)-thiolate complex, whereas the same reaction with the dimethylated ligand L^2SSL^2 does not lead to a cobalt(III)-thiolate complex (**Scheme 4.1**).[12] Finally, the redox-conversion reaction mechanism seems to be different for the cobalt-based system than for the copper-based system, as sulfur is often not coordinated in the cobalt(II)-disulfide system, preventing direct electron transfer. In Chapter 2 and Chapter 3, the reactivity is described of the cobalt-based systems with both of these ligands.[13, 14] It was found that the ligand-field strength of the exogenous ligand affects the formation of cobalt(III)-thiolate complexes. In addition, it was found that the mechanism of the redox-conversion reaction depends on the different coordination modes of the disulfide ligand as well as the exogenous bidentate ligand.[13, 14]
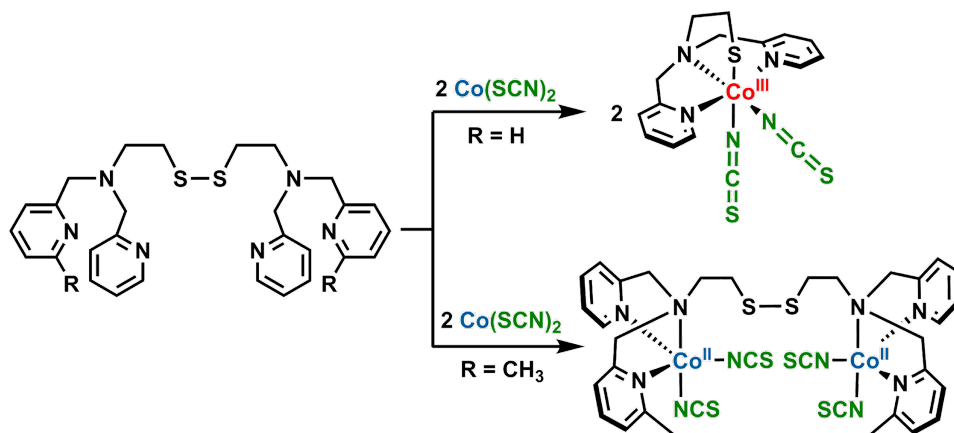
Scheme 4.1. Different reactivity of ligand L[1]SSL[1] (R=H) and L[2]SSL[2] (R=CH₃)with Co(SCN)₂ .[10,11]

To the best of our knowledge, the redox-conversion reaction using selenium-based ligands has not yet been reported. It is of importance to know whether the redox-conversion can also occur with selenolate/diselenide species, as it may give rise to a new perspective on the importance of selenium compared to sulfur in electron-transfer reactions in biology. Yet, the use of selenium as a replacement for sulfur in the redox-conversion reaction of Co(II)-diselenide to the corresponding Co(III)-selenolate complex may be challenging. The biggest challenge is that the diselenide bond has been reported to be more stable towards reduction than the disulfide bond,[15] and thus would make the redox-conversion reaction more complicated. Therefore, it is our interest to investigate the redox-conversion reaction of the selenium-based ligand L[1]SeSeL[1] by the reaction with different cobalt(II) salts or adjusting the ligand-field strength with use of external ligands.

4.2. Results

4.2.1. Synthesis of the compounds

The precursor of the ligand, selenocystamine dihydrochloride was obtained in 37% yield as a light yellow powder and characterized using ESI-MS and NMR (Figure AIII.1 and AIII.2). The ligand 2,2'-diselanediylbis(N,N-bis(pyridin-2-ylmethyl)ethan-1-amine) (L[1]SeSeL[1]) was prepared via the reductive amination of selenocystamine dihydrochloride with 2-pyridinecarboxaldehyde using sodium cyanoborohydride as reducing agent (**Scheme 4.2**). The ligand L[1]SeSeL[1] was obtained as a pale red solid in 26% yield after recrystallization.
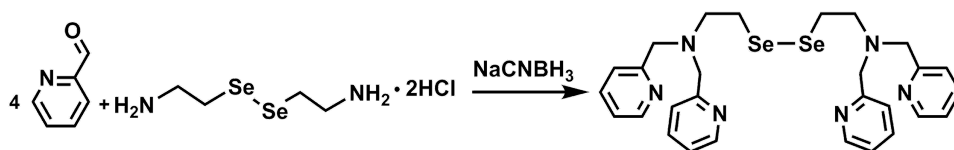
Scheme 4.2. Synthesis scheme of ligand L^1SeSeL^1.

The ESI-MS spectrum (Figure AIII.3) shows peaks at *m/z* 612.9 and 306.8 corresponding to the species $[L^1SeSeL^1 + H]^+$ and $[L^1SeSeL^1 + 2H]^{2+}$, respectively. Both ^1H-NMR spectroscopy (Figure AIII.4) and elemental analysis showed that the ligand L^1SeSeL^1 was obtained analytically pure.

Addition of the ligand L^1SeSeL^1 to a solution containing two equivalents of $CoCl_2$ in acetonitrile afforded a dark purple solution of the diselenide compound $[Co_2(L^1SeSeL^1)(Cl)_4]$ ([**1**]) (**Scheme 4.3**). Compound [**1**] was isolated as a purple solid in 50% yield. An ESI-MS spectrum of the purple powder dissolved in acetonitrile (Figure AIII.5) shows peaks at *m/z* 845.1 and 400.0 corresponding to the species $[\mathbf{1} – 2Cl^- + HCOO^-]^+$ and $[\mathbf{1} – 2Cl^-]^{2+}$, respectively, showing distinct isotopic distributions due to the presence of selenium in the compound. The presence of two high-spin cobalt(II) ions in [**1**] is indicated by the magnetic moment value of 5.98 μ_B, calculated for the dinuclear compound. The ^1H-NMR spectrum of [**1**] in CD_3CN (Figure AIII.6) shows peaks in the region between -8.64 ppm up to 88.34 ppm due to the paramagnetic nature of the compound. Compound [**1**] was proven to be analytically
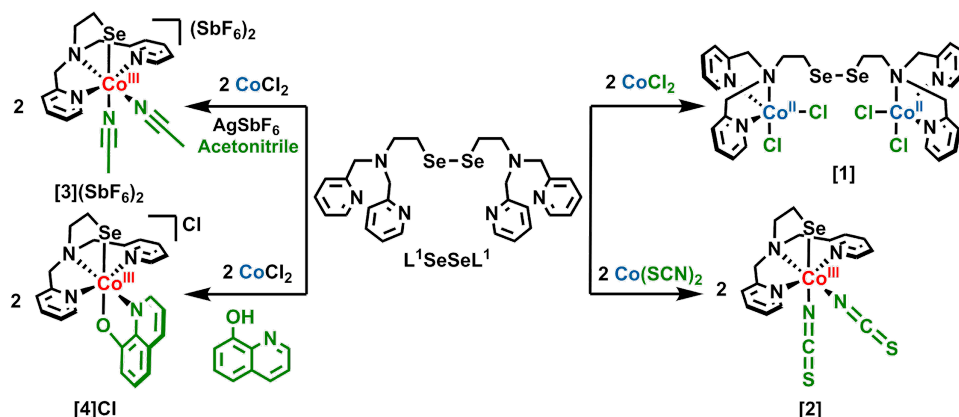
Scheme 4.3. Synthesis scheme of the complexes described in this manuscript.

pure by elemental analysis and its structure was further elucidated using single crystal X-ray diffraction.

The cobalt(III)-selenolate compound $[Co(L^1Se)(NCS)_2]$ ([2]) was obtained from a reaction of the ligand L^1SeSeL^1 with two equivalents of $Co(SCN)_2$, while the compounds $[Co(L^1Se)(MeCN)_2](SbF_6)_2$ ([3]$(SbF_6)_2$) and $[Co(L^1Se)(quin)]Cl$ ([4]Cl) were prepared via *in situ* formation of compound [1] and subsequent addition of silver hexafluoroantimonate (for [3]$(SbF_6)_2$) or 8-quinolinol (Hquin, for [4]Cl) (**Scheme 4.3**). All cobalt(III)-selenolate compounds were obtained in good yields (76%, 91%, 78%, for [2], [3]$(SbF_6)_2$, and [4]Cl, respectively), and appeared to be hygroscopic. The ESI-MS spectrum of an acetonitrile solution of [2] (Figure AIII.7) shows peaks at *m/z* 464.0 and 889.0 attributed to the species $[Co(L^1Se)(NCS)(MeCN)]^+$ and $[2\times2 - 2SCN^- + HCOO^-]^+$, respectively. The ESI-MS spectrum of an acetonitrile solution of [3]$(SbF_6)_2$ (Figure AIII.8) shows peaks at *m/z* 223.6, 410.1, 863.0, and 1054.9, corresponding to the species $[3]^{2+}$, $[3 - 2MeCN + HCOO^-]^+$, $[2\times3 - 4MeCN + 3HCOO^-]^+$, and $[2\times3 - 4MeCN + 2HCOO^- + (SbF_6)]^+$, respectively. The ESI-MS spectrum of an acetonitrile solution of compound [4]Cl (Figure AIII.9) shows a major peak at *m/z* 509.1 which can be assigned to $[4]^+$. All cobalt(III)-selenolate compounds were found to be diamagnetic based on ^{1}H-NMR spectroscopy (Figure AIII.10−AIII.16) and the determination of their magnetic moments using a magnetic susceptibility balance. Elemental analysis of the cobalt(III)-selenolate compounds show that the compounds were analytically pure (further details in Experimental Section).

4.2.2. Single Crystal X-Ray Crystallography

Single crystals of [1], [2], and [4]Cl were obtained using vapor diffusion of diethyl ether into solutions of each compound (See Experimental Section). Unfortunately, single crystals of compound [3]$(SbF_6)_2$ could not be obtained as all crystallization attempts resulted in the formation of oils. Projections of the crystal structures are depicted in **Figure 4.1**. Full crystallographic parameters are provided in Table AIII.1. The structure of [1] crystallizes in the triclinic space group *P*-1 and the asymmetric unit contains one molecule of [1] and one lattice diethyl ether solvent molecule. Both cobalt(II) centers are found to be in a distorted trigonal-bipyramidal geometry ($\tau_5 = 0.72$ for Co1 and $\tau_5 = 0.62$ for Co2, $\tau_5 = 1$ is calculated
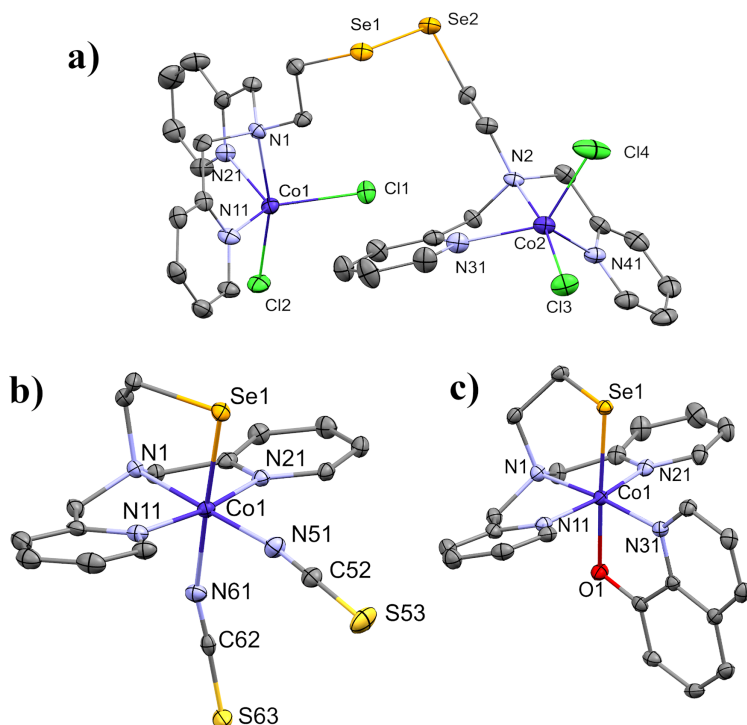
Figure 4.1. Displacement ellipsoid plots (50% probability level) of a) $[Co_2(L^1SeSeL^1)Cl_4]$ ([**1**]), b) $[Co(L^1Se)(NCS)_2]$ ([**2**]), and c) $[Co(L^1Se)(quin)]^+$ ([**4**]$^+$) at 110(2) K. Hydrogen atoms, non-coordinated anions, and lattice solvent molecules are omitted for clarity.

for a perfect trigonal-bipyramidal geometry and $\tau_5 = 0$ for perfect square pyramidal geometry).[16] Each of the cobalt(II) centers is coordinated by three nitrogen atoms from the ligand L^1SeSeL^1 and two chloride anions. The apical positions are occupied by one of the chloride ions and the tertiary amine nitrogen atom. The diselenide group is not coordinated to the Co metal centers, as observed with the disulfide group in the structure of the related compound $[Co_2(L^1SSL^1)Cl_4]$. Selected bond distances and angles are provided in **Table 4.1**. The bond distances and angles related to Co2 are similar to those of Co1. The Se1−Se2 bond distance (2.3208(7) Å) is on par with the average Se−Se bond in the reported structures (2.305 Å).[17, 18] All other bond distances and angles are also found within the expected values.

The structure of [**2**] crystallizes in the orthorhombic space group *Pbca*, and one molecule of [**2**] is found in the asymmetric unit without co-crystallized lattice solvent molecules. The cobalt center is found in a near perfect octahedral geometry, formed by the coordination of

Table 4.1. Selected bond distances and bond angles in[**1**].

Atoms	Distance (Å)	Atoms	Bond angle (°)
Se1–Se2	2.3208(7)	N1–Co1–Cl2	165.89(10)
Co1–N1	2.303(3)	N1–Co1–Cl1	91.71(10)
Co1–N11	2.074(4)	N1–Co1–N11	75.99(13)
Co1–N21	2.079(4)	N1–Co1–N21	76.95(14)
Co1–Cl1	2.2848(13)	Cl2–Co1–Cl1	102.39(5)
Co1–Cl2	2.3290(12)	Cl2–Co1–N11	95.82(10)
		Cl2–Co1–N21	97.52(11)
		N11–Co1–Cl1	122.63(12)
		N11–Co1–N21	118.18(15)
		N21–Co1–Cl1	112.65(11)

five nitrogen atoms (two from NCS⁻ ions and three from the ligand L^{1}Se⁻) and one selenolate ion. The three nitrogen donors of the ligand L^{1}Se⁻ are coordinated to the cobalt center in a meridional fashion, similar to the ligand L^{1}S⁻ in previous reports.[10, 13] As a consequence, one of the NCS⁻ ions is coordinated to *trans* to the selenolate ion and the other NCS⁻ ion is coordinated *trans* to the tertiary amine nitrogen. The structure is very similar to the structure of the previously reported compound [Co(L^{1}S)(NCS)$_2$].[10] π-Stacking interactions are present between pyridines of two neighboring molecules, the distances ranging from 3.337 Å to 3.351 Å. Short contacts of 3.693 Å are present in the unit cell between the selenolate ion and a sulfur atom of an NCS⁻ group of a neighboring molecule. A selection of bond distances and angles in [**2**] is provided in **Table 4.2**.

The structure of [**4**]Cl crystallizes in the monoclinic space group $P2_1/n$, and the asymmetric unit contains one molecule of [**4**]Cl and two disordered lattice chloroform solvent molecules. The cobalt center is found in a slightly distorted octahedral geometry, similar to [**2**]. Four nitrogen donor atoms (three from the ligand L^{1}Se⁻, one from the ligand quin⁻), one oxygen, and one selenolate donor atom are coordinated to the cobalt center. The structure of [**4**]Cl is very similar to the reported structure of its sulfur analog [Co(L^{1}S)(quin)]Cl.[14] The bond distances and bond angles are similar to the structure [Co(L^{1}S)(quin)]Cl, except for the Co1−Se1 bond distance, which is larger due to larger ionic radius of selenium compared to sulfur. Unlike [**2**], π-stacking interactions are not present in the structure of [**4**]Cl. A selection of bond distances and angles is provided in **Table 4.3**.

Table 4.2. Bond distances and bond angles in [**2**].

Atoms	Distance (Å)	Atoms	Bond angle (°)	Atoms	Bond angle (°)
Co1–Se1	2.3608(4)	Se1–Co1–N61	178.00(6)	N61–Co1–N51	89.65(8)
Co1–N1	1.9601(18)	Se1–Co1–N1	90.91(5)	N1–Co1–N11	84.87(7)
Co1–N11	1.9353(18)	Se1–Co1–N11	88.29(6)	N1–Co1–N21	84.20(7)
Co1–N21	1.9229(18)	Se1–Co1–N21	91.95(5)	N1–Co1–N51	179.27(8)
Co1–N51	1.8999(19)	Se1–Co1–N51	88.36(6)	N51–Co1–N11	95.14(8)
Co1–N61	1.9976(19)	N61–Co1–N1	91.08(7)	N51–Co1–N21	95.79(8)
		N61–Co1–N11	91.78(8)	N11–Co1–N21	169.07(8)
		N61–Co1–N21	88.35(7)		

Table 4.3. Bond distances and bond angles in [**4**]Cl.

Atoms	Distance (Å)	Atoms	Bond angle (°)	Atoms	Bond angle (°)
Co1–Se1	2.3552(3)	Se1–Co1–O1	176.94(5)	O1–Co1–N31	85.47(7)
Co1–N1	1.9527(18)	Se1–Co1–N1	90.72(5)	N1–Co1–N11	83.81(8)
Co1–N11	1.9389(18)	Se1–Co1–N11	92.80(5)	N1–Co1–N21	85.48(8)
Co1–N21	1.9333(19)	Se1–Co1–N21	88.21(5)	N1–Co1–N31	174.67(7)
Co1–N31	1.9307(18)	Se1–Co1–N31	94.37(5)	N31–Co1–N11	94.37(8)
Co1–O1	1.9770(14)	O1–Co1–N1	89.53(7)	N31–Co1–N21	96.22(8)
		O1–Co1–N11	90.26(7)	N11–Co1–N21	169.26(8)
		O1–Co1–N21	88.77(7)		

4.2.3. Solution Studies of the Cobalt(II)-Diselenide and Cobalt(III)-Selenolate Compounds

The cobalt compounds described in this Chapter are soluble in acetonitrile, except for [**2**] which is only slightly soluble in acetonitrile but fully soluble in dimethylsulfoxide. The UV-visible spectrum of each compound is depicted in **Figure 4.2**. A solution of [**1**] in acetonitrile has an intense purple color and the UV-visible spectrum shows two peaks at 558 nm ($\varepsilon = 3.15 \times 10^2$ M^{-1} cm^{-1}) and 635 nm ($\varepsilon = 2.22 \times 10^2$ M^{-1} cm^{-1}) as well as a small peak at around 850 nm, corresponding to the Co(II) *d-d* transitions in a trigonal-bipyramidal geometry.[19, 20] The UV-visible spectrum of [**1**] is very similar to that of the disulfide compound $[Co_2(L^1SSL^1)Cl_4]$ reported earlier, with no apparent shift in the absorption wavelengths.[10]

Compound [**2**] was dissolved in a mixture of acetonitrile : dimethylsulfoxide (v : v = 19 : 1), resulting in a maroon-colored solution, whereas solutions of [**3**](SbF$_6$)$_2$ and [**4**]Cl in acetonitrile are yellow. The color of the solution of [**4**]Cl is rather intense compared to those of the two other cobalt(III)-selenolate compounds. The UV-visible spectra of
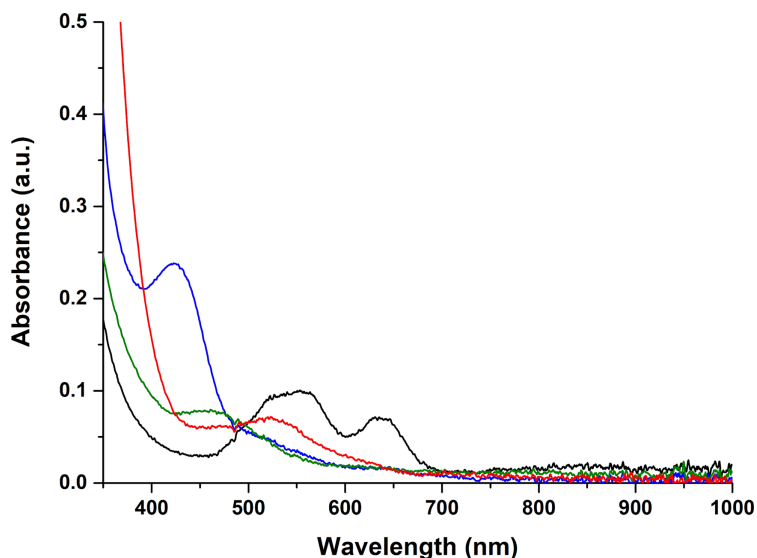
Figure 4.2. UV-visible spectra of acetonitrile solutions of [**1**] (2.5 mM concentration, black trace), [**3**](SbF$_6$)$_2$ (2 mM, green trace), [**4**]Cl (1 mM, blue trace), and a solution of [**2**] (2.5 mM, red trace) in 19 : 1 acetonitrile : dimethylsulfoxide. UV-visible spectra were taken using a transmission dip probe with path length of 1.4 mm.

cobalt(III)-selenolate compounds [**2**], [**3**](SbF$_6$)$_2$, and [**4**]Cl generally show one absorption peak. The UV-visible spectrum of [**2**] shows a weak absorption peak at 523 nm ($\varepsilon = 2.10 \times 10^2$ M^{-1} cm^{-1}), whereas [**3**](SbF$_6$)$_2$ shows similar weak absorption peak at 465 nm ($\varepsilon = 3.39 \times 10^2$ M^{-1} cm^{-1}). Such absorptions in UV-Vis spectra have been ascribed to Co(III) *d-d* transitions in an octahedral geometry.[21, 22] The spectrum of [**4**]Cl shows one strong absorption peak at 422 nm ($\varepsilon = 1.70 \times 10^3$ M^{-1} cm^{-1}) tentatively ascribed to a ligand-to-metal charge transfer from the quin$^-$ ligand to the cobalt center, similar to the spectrum of [Co(L^{1}S)quin]Cl described in Chapter 3.[14]

4.2.4. The Ligand-Field Splitting Energy of Selenolate Compounds

In Chapters 2 and 3, the ligand-field strength of exogenous ligands has been shown to affect the conversion of cobalt(II)-disulfide to cobalt(III)-thiolate species; the ligand-field strength was estimated from the MO energy levels using DFT computations.[13, 14] In this Chapter, a similar approach was taken to approximate the ligand-field strength of the ligand L^{1}SeSeL^1. The structures of [**2**], [**3**]$^{2+}$, as well as [**4**]$^+$ were optimized using ZORA-OPBE/TZP all-electron basis set. The equilibrium geometries show satisfactory results, as shown by

similarities of the bond lengths of [**2**] and [**4**]$^+$ with the experimental values from the crystal structures (**Table 4.4**). The largest bond length deviation of 0.024 Å is found in the calculated Co1−N11 bond in [**2**]$^+$. Other calculated bond lengths deviate by about 0.002 Å to 0.024 Å.

The *d*-orbital splitting energy was estimated using the method described in Chapter 2.[13] Again we found the five non-degenerate molecular orbitals with the highest contribution from Co *d*-orbitals (Figure AIII.17−AIII.19). These five orbitals approximately form two sets of orbitals in agreement with an octahedral splitting according to ligand-field theory. As the two sets of orbitals also contain contributions from the ligands in varying amounts, the *d*-orbital splitting energy can only be estimated in a rather qualitative way from the energy difference of the highest and the lowest orbital of this set. The results are compared to the sulfur analogs of [**2**], [**3**]$^{2+}$, and [**4**]$^+$ in **Figure 4.3**. The energy differences between the highest and lowest MO with large *d*-orbital contributions in compounds [**2**], [**3**]$^{2+}$, and [**4**]$^+$ are qualitatively smaller than those of their corresponding sulfur analogs. Therefore, replacement of sulfur with selenium apparently resulted in a slightly weaker ligand-field strength of the L^{1}Se ligand. The differences between the *d*-orbital energies of the selenolate compounds with those of the sulfur analogs seems to follow a trend, i.e. the difference in energy of the highest and lowest MO comprising major *d*-orbital contribution between the Se and S compounds becomes smaller from [**2**] via [**3**]$^{2+}$ to [**4**]$^+$. This apparent trend seems to be related to the ligand-field strength of the auxiliary ligands, from the weakest to the strongest in the order of NCS$^-$ < CH$_3$CN < quin$^-$, indicating that the contribution of the auxiliary ligand in the overall ligand-field splitting energy becomes dominant.[23, 24]

Table 4.4. Comparison between experimental and DFT bond distances in [**2**] and in [**4**]$^+$.

Atoms	Bond Distance in [**2**] (Å)		Atoms	Bond Distance in [**4**]$^+$ (Å)	
	XRD	DFT		XRD	DFT
Co1–Se1	2.3608(4)	2.358	Co1–Se1	2.3552(3)	2.361
Co1–N1	1.9601(18)	1.966	Co1–N1	1.9527(18)	1.967
Co1–N11	1.9353(18)	1.911	Co1–N11	1.9389(18)	1.925
Co1–N21	1.9229(18)	1.906	Co1–N21	1.9333(19)	1.925
Co1–N51	1.8999(19)	1.846	Co1–N31	1.9307(18)	1.921
Co1–N61	1.9976(19)	1.962	Co1–O1	1.9770(14)	1.958
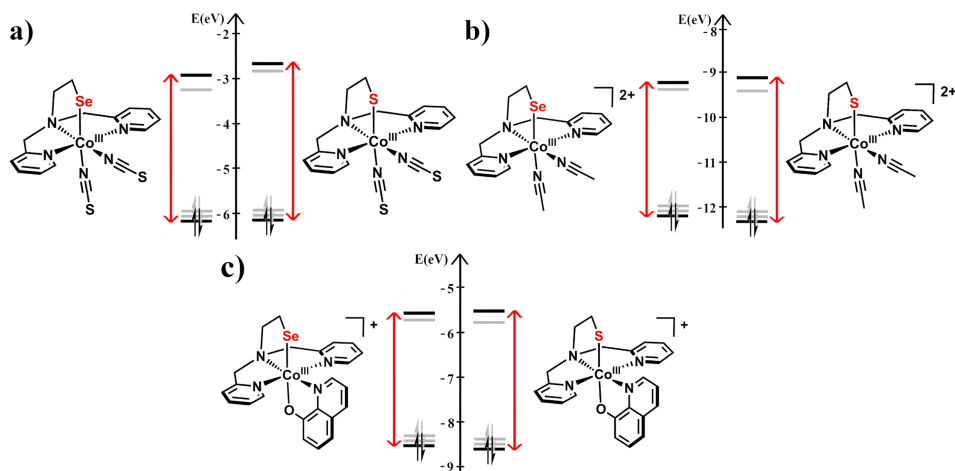
Figure 4.3. Comparison of the estimated *d*-orbital splitting energies of a) [**2**], b) [**3**]$^{2+}$, and c) [**4**]$^{+}$ with its corresponding sulfur analog.

4.3. Discussion

The disulfide ligand L^{1}SSL^1 in copper(I) or cobalt(II) complexes has been reported to facilitate intramolecular electron transfer with the metal center, in a so-called redox-conversion reaction.[10, 25, 26] To the best of our knowledge, this redox-conversion reaction has never been reported for a selenium-based ligand. Therefore, our study of the potential redox-conversion cobalt(II)-diselenide compounds started with the preparation of the new ligand L^{1}SeSeL^1, which structurally resembles the sulfur analog L^{1}SSL^1. Our results show that indeed redox-conversion reactions can also take place using a diselenide ligand.

The reaction of L^{1}SeSeL^1 with cobalt(II) chloride in acetonitrile afforded the cobalt(II)-diselenide compound [**1**], which resembles the reported compound [Co$_2$(L^{1}SSL^1)Cl$_4$], having very similar spectroscopic properties.[10] The reaction with cobalt(II) thiocyanate resulted in the cobalt(III)-selenolate complex [**2**], similar to [Co(L^{1}S)(NCS)$_2$]. However, the ESI-MS spectrum of a solution of [**2**] (Figure AIII.7) shows signals attributed to the apparent formation of the diselenide dimer of the compound. Other spectroscopic techniques that were used to characterize [**2**] showed that in the solid state compound [**2**] is pure, but indicate that in solution [**2**] easily reverts to a diselenide-cobalt(II) compound.

Like its sulfur analog, [1] undergoes a redox-conversion reaction upon the addition of an external trigger, as shown by the formation of [3](SbF$_6$)$_2$ and [4]Cl after treatment of *in situ* formed [1] with a silver salt or quinolinol. Full conversion of [1] to [3](SbF$_6$)$_2$ was achieved successfully. In principle, this reactivity is similar to the formation of [Co(L^{1}S)(MeCN)$_2$]$^{2+}$ from the reaction of L^{1}SSL^1 with [Co(MeCN)$_6$](BF$_4$)$_2$,[10] or from the dissolution of [Co$_2$(L^{1}SSL^1)(PF$_2$O$_2$)$_2$](PF$_6$)$_2$ in acetonitrile.[12] Acetonitrile will coordinate to the cobalt center and has sufficiently strong ligand-field effect to trigger the conversion, as long as there is no strongly coordinating ligand or anion. Despite the observed formation of [3](SbF$_6$)$_2$, this compound likely is unstable in solution. In the ^{1}H-NMR spectrum of [3](SbF$_6$)$_2$, partial decomposition of the cobalt(III)-selenolate complex is indicated by the presence of several peaks in the aromatic region (6.60−7.25 ppm) as well as at 2.75 ppm, which possibly arise from degradation of the ligand. The instability of the cobalt(III)-selenolate compounds can be explained by the more negative reduction potential of the diselenide bond than that of the disulfide bond;[27] re-oxidation of selenolate to the diselenide (dimer) appears to be relatively easy of as indicated by the presence of peaks assigned to dimeric compounds in the ESI-MS spectra of [2] and [3](SbF$_6$)$_2$. Nevertheless, full conversion of [1] to [4]Cl was achieved in a clean manner with the strong-field ligand quinolinolate.

Based on the experimental results it seems that the presence of selenium in the ligand causes a smaller ligand-field splitting than sulfur. Although the ligand-field splitting energy of the selenium-based ligand may be smaller than that of the sulfur analog, it appears that this can be counteracted by the auxiliary ligand. This assumption is supported by our DFT computations, with the results shown in **Figure 4.3**: the difference in energy of the highest and lowest MO orbital with major *d*-orbital contribution of the selenolate compounds compared to the thiolate analogs becomes smaller in the order of NCS$^-$, CH$_3$CN, and quin$^-$. These results indicate that indeed the ligand-field strength contribution of these auxiliary ligand overcomes the smaller ligand-field splitting energy of the selenium donor atom. The clean formation of [4]Cl shows that with the strong-field ligand quin$^-$ full conversion can be achieved. Generally, our results show the similarities and differences in redox-conversion reactivity of the diselenide ligand L^{1}SeSeL^1 compared to L^{1}SSL^1.

4.4. Conclusion

The diselenide L^1SeSeL^1 analog of the disulfide ligand L^1SSL^1 was successfully synthesized. Reaction of the ligand L^1SeSeL^1 with cobalt(II) salts resulted in the formation of either cobalt(II)-diselenide compound [**1**] with chloride ions or the cobalt(III)-selenolate compound [**2**] with thiocyanate ions. The redox-conversion of cobalt(II)-diselenide compound [**1**] to cobalt(III)-selenolate compounds [**3**]$(SbF_6)_2$ or [**4**] has been proven to be successful, using the strategies employed in previous reports for L^1SSL^1. The cobalt(III)-selenolate compounds [**2**] and [**3**]$(SbF_6)_2$ appear to be relatively unstable in solution, the compounds partially revert to a diselenide compound or decompose. However, formation of [**4**] is clean, showing that the ligand-field strength of the auxiliary ligand can overpower the weaker ligand-field exerted by the selenium-based ligand. Overall, our results indicate that cobalt compounds with the ligand L^1SeSeL^1 show reactivity that is very similar to the sulfur analogs. The selenium-based ligand appears to exert a slightly lower ligand-field strength, which is not unexpected due to the stronger pi-donating effects of the larger lone pairs on selenium. These studies can be directed to investigate the kinetics of the reaction, or derivatization of the ligand L^1SeSeL^1, which may give insights not only in the diselenide to selenolate conversion, but also their efficiency in natural systems.

4.5. Experimental Section

4.5.1. General

All reagents were purchased from commercial sources and used as received unless noted otherwise. Deoxygenated solvents used were obtained by the freeze-pump-thaw method followed by drying the solvents using appropriate size of molecular sieves. The synthesis of the cobalt compounds was performed using standard Schlenk-line techniques under argon atmosphere. ^{1}H NMR spectra were recorded on a Bruker 300 DPX spectrometer at room temperature. Mass spectra were recorded on a Thermo Scientific MSQ Plus or Shimadzu LCMS 2020 mass spectrometer with electrospray ionization (ESI) method, formic acid was added to the eluting solvent with 1% final concentration. Simulated mass spectra were generated using the mMass (version 5.5.0) software.[28] IR spectra were obtained using a PerkinElmer Spectrum Two System equipped with Universal ATR module containing diamond crystal for single reflection (scan range 400–4000 cm^{-1}, resolution 4 cm^{-1}). Analyses of bond distances and angles of the structures were performed using the Mogul

module in Mercury (version 4.3.1) software.[29] UV-visible spectra were collected using a transmission dip probe with variable path lengths and reflection probe on an Avantes AvaSpec-2048 spectrometer and using an Avalight-DH-S-Bal light source. Elemental analyses were performed by the Microanalytical Laboratory Kolbe in Germany.

4.5.2. Single crystal X-ray crystallography

All reflection intensities were measured at 110(2) K using a SuperNova diffractometer (equipped with Atlas detector) with Mo *K*α radiation (λ = 0.71073 Å) under the program CrysAlisPro (Version CrysAlisPro 1.171.39.29c, Rigaku OD, 2017). The same program was used to refine the cell dimensions and for data reduction. The structure was solved with the program SHELXS-2018/3 and was refined on F^2 with SHELXL-2018/3.[30] Numerical absorption correction based on Gaussian integration over a multifaceted crystal model was applied using CrysAlisPro. The temperature of the data collection was controlled using the system Cryojet (manufactured by Oxford Instruments). The H atoms were placed at calculated positions using the instructions AFIX 23, AFIX 43 or AFIX 137 with isotropic displacement parameters having values 1.2 or 1.5 U_{eq} of the attached C atoms. The crystal structures of [**1**] and [**2**] are ordered. For compound [**4**]Cl, the two lattice chloroform molecules were found to be disordered over either two or three orientations, and the occupancy factors for the major / minor components of the disorder can be retrieved from the .cif file.

4.5.3. Computational methods

All calculations were performed with density functional theory using the Amsterdam Density Functional (ADF) program version 2017.103.[31] Geometries and energies were computed using OPBE functional.[32] Molecular orbitals (MO) were expanded in a large uncontracted TZP Slater type orbital (STO) basis set.[33] Scalar relativistic effects were accounted for using the zeroth order regular approximation (ZORA).[34] The stationary points were checked to be minima at potential energy surface using vibrational analysis. The calculations for all cobalt(III)-selenolate compounds were done with $S = 0$ (low-spin cobalt(III) center). The *d*-orbital splitting energies were estimated using similar method described in Chapter 2.[13]

4.5.4. Synthesis of the compounds

Selenocystamine dihydrochloride (C₄H₁₂N₂Se₂·2HCl)

Caution: Selenium and its derivative listed here are extremely toxic and exudes foul smell, one should ensure proper ventilation and personal protective equipment at all times.

H_2N ⌒ Se ⌒ Se ⌒ NH_2·2HCl
Selenocystamine dihydrochloride
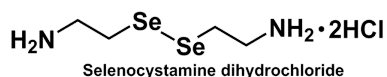
A 3-necked round-bottomed flask was purged with argon before the reaction was started. Into the 3-necked round-bottomed flask, selenium powder (4.75 g, 60 mmol) was added, followed by 25 mL of demineralized water (previously bubbled with argon). The flask was then fitted with a gas outlet and an addition funnel. In another flask, 15.0 grams of lead(II) acetate trihydrate was dissolved in 300 mL demineralized water. The solution of lead(II) acetate was added to a gas washing bottle, keeping the solution level above the bubbler to detect any gas formation. The gas outlet of the reaction flask was connected to the inlet of the gas washing bottle. In a separate flask, 4.54 grams of NaBH₄ (120 mmol, 2 equiv.) was dissolved in 25 mL demineralized water, bubbled with argon for 20 minutes, and the solution was quickly transferred to the addition funnel. The colloidal selenium mixture was stirred and NaBH₄ was added slowly to keep the bubbling at a moderate pace. During the addition of NaBH₄, the solution in the gas-trap apparatus changed color from colorless to black, indicating the formation of PbSe species. The grey colloidal selenium mixture changed to a clear red solution during the addition of NaBH₄ and ultimately to a light yellow solution after full addition of NaBH₄. The solution was stirred for 10 minutes, followed by addition of selenium powder (4.75 g, 60 mmol) in four portions over the course of 30 minutes. The resulting dark red-colored solution was stirred for another 20 minutes. While stirring, 2-chloroethylamine hydrochloride (13.9 g, 120 mmol, 2 equiv.) was dissolved in 30 mL NaOH 5 M, which was deoxygenated by bubbling with argon for 20 minutes. This solution was transferred to the addition funnel, then added dropwise to the reaction mixture. The gas outlet and the addition funnel was removed after the addition, and the resulting solution was stirred overnight at room temperature under an argon atmosphere.

The reaction mixture was transferred into a separating funnel, then extracted with 5×100 mL CHCl₃. The organic layer was collected and subsequently dried over MgSO₄. The organic layer was filtered and concentrated using a rotary evaporator. The resulting oil (15.34 g) was

dissolved in 100 mL methanol and 100 mL ethyl acetate. Anhydrous HCl in diethyl ether (65 mL) was added slowly to the solution, and the reaction mixture was stirred for an hour. After an hour, the mixture was concentrated using a rotary evaporator. The resulting solid (12.13 g) was dissolved in the minimum amount of methanol, and ethyl acetate was added slowly until the formation of precipitates occurred. Filtration of the light yellow solid and subsequent washing with diethyl ether followed by drying in air gave a light yellow powder as the product. Yield = 7.05 g, (37%). ESI-MS found (calcd.) for [M+H]$^+$ *m/z* 248.9 (248.94). ^{1}H-NMR (300 MHz, (CD$_3$)$_2$SO, RT), δ(ppm): 8.24 (s, 4H, amine N**H$_2$**), 3.35 (s, 8H, NH$_2$-C**H$_2$**-C**H$_2$**-Se-).

2,2'-Diselanediylbis(N,N-bis(pyridin-2-ylmethyl)ethan-1-amine) (L^{1}SeSeL^1)

In a 500 mL round-bottom flask, selenocystamine dihydrochloride (3.22 grams, 10.1 mmol) was dissolved in 150 mL methanol, resulting in a red-colored solution. Into the solution, 2-pyridinecarboxaldehyde (4 mL, 42 mmol, 4 equiv.) was added and the reaction mixture was stirred for one hour. Then, sodium cyanoborohydride (2.95 g, 47 mmol, 4.7 equiv.) was added in four portions, the first two portions were added over the course of 15 minutes. The remaining portions were added after stirring the solution for 12 hours, over the course of 15 minutes. The color of the solution turned yellow-green, and the solution was stirred for another three days. The reaction was quenched after three days by addition of 37% HCl until pH =1. The solvent was removed using a rotary evaporator, resulting in a yellow oil, which was dissolved in 50 mL NaOH (10 M). The solution was transferred into a separatory funnel and extracted with 3×100 mL CHCl$_3$. The organic layer was collected, dried over MgSO$_4$. Filtration of the solids and removal of the solvent using a rotary evaporator resulted in a red-orange oil, which was carefully treated with 10 mL 70% HClO$_4$. Absolute ethanol (400 mL) was added to the mixture, the initially formed turbid solution turned clear orange after 3 hours of stirring. The orange-colored solution was then removed, resulting in a dark red sticky oil, which was converted back to the free base using 50 mL NaOH (10 M). The solution was transferred to a separatory funnel and extracted again with 3×100 mL CHCl$_3$. The organic layer was collected, dried over MgSO$_4$, filtered, and then the solvent was removed using a rotary evaporator. The resulting crude product (red oil) was

crystallized using 300 mL petroleum ether under overnight reflux condition. After reflux, the petroleum ether solution was transferred to an erlenmeyer flask and stored in a refrigerator for several days until a pale red precipitate formed. The solids were collected by filtration, dried in air and weighed. Yield = 1.6 g (26%). ESI-MS found (calcd.) for $[L^1SeSeL^1 + H]^+$ m/z 612.9 (613.1) $[L^1SeSeL^1 + 2H]^{2+}$ m/z 306.8 (307.06). ^{1}H-NMR (300 MHz, CD$_3$CN, RT), δ(ppm): 2.79-2.84 (t, 4H, N-CH$_2$-**CH$_2$**-Se), 3.04-3.08 (t, 4H, N-C**H$_2$**-CH$_2$-Se), 3.78 (s, 8H, N-C**H$_2$**-Py), 7.17-7.22 (ddd, 4H, Py-**H$_5$**), 7.54-7.56 (d, 4H, Py-**H$_3$**), 7.68-7.74 (td, 4H, Py-**H$_4$**), 8.46-8.49 (m, 4H, Py-**H$_6$**). Elemental analysis (%) for L^{1}SeSeL^1 (C$_{28}$H$_{32}$N$_6$Se$_2$) calcd. C, 55.09; H, 5.28; N, 13.77; found C, 54.96; H, 5.31; N, 13.60.

$[Co_2(L^1SeSeL^1)(Cl)_4]$ ([1])
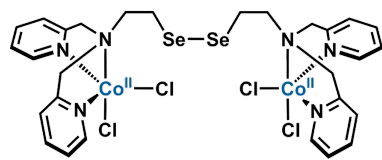
[Co$_2$(L^{1}SeSeL^1)(Cl)$_4$]

The ligand L^{1}SeSeL^1 (65.8 mg, 0.108 mmol) was dissolved in 5 mL dry and deoxygenated acetonitrile. Anhydrous CoCl$_2$ (28.0 mg, 0.216 mmol, 2 equiv.) was added into the solution of L^{1}SeSeL^1 and the color immediately turned dark purple. The solution was stirred for three hours and then concentrated *in vacuo* until approximately 1 mL was left in the flask. Diethyl ether (12 mL) was subsequently added into the flask, affording a purple precipitate. The precipitate was filtered, washed twice with diethyl ether, then dried *in vacuo*. The dried purple powder was collected and weighed. The purple powder is air stable. Yield = 46.6 mg (50%). Purple platelike single crystals of [**1**] were grown using vapor diffusion of diethyl ether into an acetonitrile solution of [**1**]. IR (neat, cm^{-1}): 3065vw, 3029vw, 2964vw, 2916w, 2848vw, 1606vs, 1571m, 1480s, 1442vs, 1380w, 1367w, 1308m, 1292m, 1260m, 1226vw, 1156m, 1099m, 1083m, 1053s, 1023vs, 981w, 961m, 900w, 862w, 844w, 766vs, 736m, 683w, 649m, 513w, 477m, 417s. ESI-MS found (calcd.) for [**1** – 2Cl$^-$]$^{2+}$ m/z 400.0 (399.95), for [**1** – 2Cl$^-$ + HCOO$^-$]$^+$ m/z 845.1 (844.90). Elemental analysis (%) for [**1**] (C$_{28}$H$_{32}$Co$_2$N$_6$Se$_2$Cl$_4$) calcd. C, 38.65; H, 3.71; N, 9.66; found C, 38.49; H, 3.69; N, 9.46.

[Co(L^{1}Se)(NCS)$_2$] ([2])

[Co(L^{1}Se)(NCS)$_2$]

Preparation of [**2**] was similar to compound [**1**], using Co(SCN)$_2$ instead of CoCl$_2$. Ligand L^{1}SeSeL^1 (68.0 mg, 0.111 mmol) in dry and deoxygenated acetone was mixed with Co(SCN)$_2$ (39.0 mg, 0.222 mmol, 2 equiv.). A purple powder was obtained. Yield = 81.0 mg (76%). Dark red single crystals of [**2**] were grown using vapor diffusion of diethyl ether into a 1:1 acetonitrile:methanol solution of [**2**] over the course of three days. IR (neat, cm^{-1}): 2969w, 2900w, 2057vs, 1692w, 1606s, 1572m, 1482m, 1443s, 1366m, 1307m, 1291m, 1250m, 1225w, 1155m, 1100m, 1079m, 1054s, 1024s, 973m, 957m, 901w, 862w, 841w, 763vs, 734m, 722m, 650m, 512w, 475s, 446w, 418s. ^{1}H-NMR (300 MHz, CD$_3$CN, RT), δ(ppm): 3.22-3.30 (m, 2H, N-C**H$_2$**-CH$_2$-Se), 4.18-4.24 (d, 2H, N-C**H$_2$**-py), 4.92-4.97 (d, 2H, N-C**H$_2$**-py), 7.44-7.47 (d, 2H, Py-**H$_3$**), 7.54-7.59 (t, 2H, Py-**H$_5$**), 7.96-8.01 (t, 2H, Py-**H$_4$**), 8.47-8.49 (d, 2H, Py-**H$_6$**), the proton signal of N-CH$_2$-C**H$_2$**-Se is obscured by the solvent peak at around 2.12-2.25 ppm, but was assigned using ^{1}H-COSY spectrum. ESI-MS found (calcd.) for [**2** – SCN$^-$ + MeCN]$^+$ *m/z* 463.9 (463.99), for [2×**2** – 2SCN$^-$ + HCOO$^-$]$^+$ *m/z* 889.0 (888.92). Elemental analysis (%) for [**2**] (C$_{16}$H$_{16}$CoN$_5$S$_2$Se) + 0.3H$_2$O calcd. C, 39.56; H, 3.44; N, 14.42; found C, 39.46; H, 3.31; N, 14.31.

## [Co(L^{1}Se)(MeCN)$_2$](SbF$_6$)$_2$ ([3](SbF$_6$)$_2$)

[Co(L^{1}Se)(MeCN)$_2$] (SbF$_6$)$_2$

The ligand L^{1}SeSeL^1 (61.0 mg, 0.1 mmol) was dissolved in 5 mL dry and deoxygenated acetonitrile. Anhydrous CoCl$_2$ (26.0 mg, 0.2 mmol, 2 equiv.) was added and the resulting purple-colored solution was stirred for 30 minutes. Silver hexafluoridoantimonate (143.7 mg, 0.42 mmol, 4.2 equiv.) was added and the resulting solution turned brown with some white precipitate, presumably AgCl. The resulting suspension was stirred for 2 hours, followed by filtration into a clean schlenk flask. The brown filtrate was concentrated until approximately 1 mL. Diethyl ether (12 mL) was added into the flask resulting in the formation of a dark

brown oil. The oil was separated by careful removal of the diethyl ether using a syringe, then the oil was washed twice with diethyl ether, and dried *in vacuo*. The oil quickly solidified and turned into a semi-crystalline powder. Yield = 166.8 mg (91%). IR (neat, cm^{-1}): 3516s, 3466s, 3262m, 3201m, 3122m, 2988m, 2972m, 2901m, 1624m, 1612m, 1573w, 1538w, 1471m, 1446m, 1411w, 1394w, 1378w, 1290w, 1249w, 1231w, 1165w, 1056m, 1026m, 973w, 896vw, 880vw, 838w, 821vw, 765s, 727s, 655vs, 624vs, 480m, 452m, 421m. ESI-MS found (calcd.) for [**3**]$^{2+}$ *m/z* 223.6 (223.52), for [**3** – 2MeCN + HCOO$^-$]$^+$ *m/z* 410.1 (410.98), for a dimer [2×**3** – 4MeCN + 3HCOO$^-$]$^+$ *m/z* 863.0 (862.96), and for [2×**3** – 4MeCN + 2HCOO$^-$ + SbF$_6^-$]$^+$*m/z* 1054.9 (1054.86). ^{1}H-NMR (300 MHz, CD$_3$OD, RT), δ(ppm): 2.83-2.86 (m, 2H, N-CH$_2$-**CH$_2$**-Se), 3.07-3.11 (m, 2H, N-**CH$_2$**-CH$_2$-Se), 3.81 (s, 4H, N-**CH$_2$**-py), 7.42-7.47 (t, 4H, Py-**H$_3$** and Py-**H$_5$**), 7.85-7.91 (t, 2H, Py-**H$_4$**), 8.62-8.64 (d, 2H, Py-**H$_6$**),. The compound is not stable in solution, as is apparent from impurities detected at 2.75 (s, 1H), 6.38-6.44 (t, 0.5H), 6.72-6.75 (d, 0.5H), 6.89-6.91 (d, 0.5H), 7.19-7.24 (t, 0.5H). Elemental analysis (%) for [**3**](SbF$_6$)$_2$ (C$_{18}$H$_{22}$CoF$_{12}$N$_5$Sb$_2$Se) calcd. C, 55.09; H, 5.28; N, 13.77; found C, 54.96; H, 5.31; N, 13.60.

[Co(L^{1}Se)(quin)]Cl ([4]Cl)
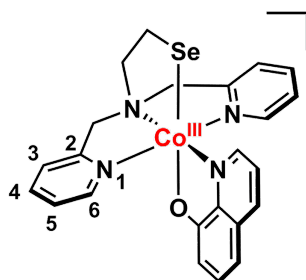
[Co(L^{1}Se)(quin)]Cl

The ligand L^{1}SeSeL^1 (61.19 mg, 0.1 mmol) and anhydrous CoCl$_2$ (26.0 mg, 0.2 mmol, 2 equiv.) were dissolved in 5 mL dry and deoxygenated methanol, affording a solution of [**1**] as described above. Into this solution, 8-quinolinol (28.88 mg, 0.2 mmol, 2 equiv.) was added. The solution turned from purple into brown and the solution was stirred for another three hours. The solution was concentrated until approximately 1 mL, diethyl ether (12 mL) was added to the concentrated solution, which resulted in the formation of a brown precipitate. The brown precipitate was filtered, washed twice with diethyl ether, then dried *in vacuo*, and weighed. Yield = 85.19 mg (78%). Dark brown single crystals of [**4**]Cl were grown using vapor diffusion of diethyl ether into a chloroform solution of [**4**]Cl. IR (neat, cm^{-1}): 3361b, 2984w, 2969w, 2050vw, 1657s, 1632s, 1571m, 1498s, 1463s, 1408s, 1374s, 1321s, 1284m, 1222w, 1173w, 1156w, 1110m, 1053w, 1008m, 980w, 876w, 831s, 803w, 749s, 703s, 663w, 643w, 552w, 531m, 516w 501w, 454w, 420w. ESI-MS found (calcd.) for

[**4**]$^+$ *m/z* 509.1 (509.03) and its isotopic pattern. ^{1}H-NMR (300 MHz, CD$_3$CN, RT), δ(ppm): 3.61-3.63 (t, 2H, N-C**H$_2$**-CH$_2$-Se), 4.54-4.59 and 5.45-5.50 (d, d, total 4H, N-C**H$_2$**-Py), 6.86-6.89 (dd, 1H, ortho-C**H**-O(quin)), 7.02-7.05 (dd, 1H, para-C**H**-O(quin)), 7.10-7.15 (t, 2H, Py-**H$_5$**), 7.34-7.39 (m, 3H, Py-**H$_3$** and meta-C**H**-O(quin)), 7.46-7.49 (d, 2H, Py-**H$_4$**), 7.74 (dd, 1H, meta-C**H**-N(quin)), 7.79-7.85 (td, 2H, Py-**H$_6$**), 8.45-8.48 (d, 1H, para-C**H**-N(quin)), 9.02-9.04 (d, 1H, ortho-C**H**-N(quin)), the proton signal of N-CH$_2$-C**H$_2$**-Se is obscured by the solvent peak at around 2.15-2.25 ppm, but was assigned using ^{1}H-COSY spectrum. Elemental analysis (%) for [**4**]Cl (C$_{23}$H$_{22}$CoN$_4$OSeCl) + H$_2$O calcd. C, 49.17; H, 4.31; N, 9.97; found C, 48.77; H, 3.97; N, 9.89.

4.6. References

1. Gennari, M. and Duboc, C. *Acc. Chem. Res.* **2020**, 53 (11), 2753-2761.
2. Hu, C., Yu, Y. and Wang, J. *Chem. Commun.* **2017**, 53 (30), 4173-4186.
3. Martin, D. R. and Matyushov, D. V. *Sci. Rep.* **2017**, 7, 1-11.
4. Bock, A., Forchhammer, K., Heider, J., Leinfelder, W., Sawers, G., Veprek, B. and Zinoni, F. *Mol. Microbiol.* **1991**, 5 (3), 515-520.
5. Cone, J. E., Martindelrio, R., Davis, J. N. and Stadtman, T. C. *Proc. Natl. Acad. Sci. U.S.A.* **1976**, 73 (8), 2659-2663.
6. Reich, H. J. and Hondal, R. J. *ACS Chem. Biol.* **2016**, 11 (4), 821-841.
7. Takei, T., Ando, T., Takao, T., Ohnishi, Y., Kurisu, G., Iwaoka, M. and Hojo, H. *Chem. Commun.* **2020**, 56 (91), 14239-14242.
8. Steinmann, D., Nauser, T. and Koppenol, W. H. *J. Org. Chem.* **2010**, 75 (19), 6696-6699.
9. Huber, R. E. and Criddle, R. S. *Arch. Biochem. Biophys.* **1967**, 122 (1), 164-173.
10. Jiang, F., Siegler, M. A., Sun, X., Jiang, L., Fonseca Guerra, C. and Bouwman, E. *lnorg. Chem.* **2018**, 57 (15), 8796-8805.
11. Ording-Wenker, E. C. M., van der Plas, M., Siegler, M. A., Bonnet, S., Bickelhaupt, F. M., Fonseca Guerra, C. and Bouwman, E. *lnorg. Chem.* **2014**, 53 (16), 8494-8504.
12. Jiang, F., Marvelous, C., Verschuur, A. C., Siegler, M. A., Teat, S. J. and Bouwman, E. *Inorg. Chim. Acta* **2022**, 120880.
13. Marvelous, C., de Azevedo Santos, L., Siegler, M. A., Fonseca Guerra, C. and Bouwman, E. *Dalton Trans.* **2022**, 51, 8046-8055.
14. Marvelous, C., de Azevedo Santos, L., Siegler, M. A., Fonseca Guerra, C. and Bouwman, E. **2022**, submitted
15. Yue, D., Cheng, G., He, Y., Nie, Y., Jiang, Q., Cai, X. and Gu, Z. *J. Mater. Chem. B* **2014**, 2 (41), 7210-7221.
16. Addison, A. W., Rao, T. N., Reedijk, J., Vanrijn, J. and Verschoor, G. C. *J. Chem. Soc., Dalton Trans.* **1984**, (7), 1349-1356.
17. Singh, P., Singh, H. B. and Butcher, R. J. *J. Organomet. Chem.* **2018**, 876, 1-9.
18. Sureshkumar, D., Gunasundari, T., Saravanan, V. and Chandrasekaran, S. *Tetrahedron Lett.* **2007**, 48 (4), 623-626.
19. Chan, S. L.-F., Lam, T. L., Yang, C., Lai, J., Cao, B., Zhou, Z. and Zhu, Q. *Polyhedron* **2017**, 125, 156-163.
20. Massoud, S. S., Broussard, K. T., Mautner, F. A., Vicente, R., Saha, M. K. and Bernal, I. *Inorg. Chim. Acta* **2008**, 361 (1), 123-131.
21. Basolo, F. *J. Am. Chem. Soc.* **1950**, 72 (10), 4393-4397.
22. Matsuoka, N. *Bull. Chem. Soc. Jpn.* **1986**, 59 (7), 2151-2155.

23. Shimura, Y. and Tsuchida, R. *Bull. Chem. Soc. Jpn.* **1956**, 29 (3), 311-316.
24. Ishii, T., Tsuboi, S., Sakane, G., Yamashita, M. and Breedlove, B. K. *Dalton Trans.* **2009**, (4), 680-7.
25. Itoh, S., Nagagawa, M. and Fukuzumi, S. *J. Am. Chem. Soc.* **2001**, 123 (17), 4087-4088.
26. Ueno, Y., Tachi, Y. and Itoh, S. *J. Am. Chem. Soc.* **2002**, 124 (42), 12428-12429.
27. Besse, D., Siedler, F., Diercks, T., Kessler, H. and Moroder, L. *Angew. Chem. Int. Ed.* **1997**, 36 (8), 883-885.
28. Strohalm, M., mMass - Open Source Mass Spectrometry Tool. www.mmass.org
29. Macrae, C. F., Sovago, I., Cottrell, S. J., Galek, P. T. A., McCabe, P., Pidcock, E., Platings, M., Shields, G. P., Stevens, J. S., Towler, M. and Wood, P. A. *J. Appl. Crystallogr.* **2020**, 53, 226-235.
30. Sheldrick, G. M. *Acta Crystallogr. Sect. A: Found. Crystallogr.* **2008**, 64, 112-122.
31. ADF2017.107. SCM Theoretical Chemistry, Vrije Universiteit: Amsterdam, The Netherlands, www.scm.com
32. Swart, M., Ehlers, A. W. and Lammertsma, K. *Mol. Phys.* **2004**, 102 (23-24), 2467-2474.
33. Van Lenthe, E. and Baerends, E. J. *J. Comput. Chem.* **2003**, 24 (9), 1142-1156.
34. Van Lenthe, E., Baerends, E. J. and Snijders, J. G. *J. Chem. Phys.* **1994**, 101 (11), 9783-9792.